Metabolic Rhythms of the Cyanobacterium *Cyanothece* sp. ATCC 51142 Correlate with Modeled Dynamics of Circadian Clock

Jan Červený[*] and Ladislav Nedbal[*,†]

[*]*Institute of Systems Biology and Ecology, Academy of Sciences CR, Nové Hrady, Czech Republic, and* [†]*Photon Systems Instruments, Ltd., Brno, Czech Republic*

Abstract These experiments aim to reveal the dynamic features that occur during the metabolism of the unicellular, nitrogen fixing cyanobacterium *Cyanothece* sp. when exposed to diverse circadian forcing patterns (LD 16:8, LD 12:12, LD 8:16, LD 6:6). The chlorophyll concentration grew rapidly from subjective morning when first illuminated to around noon, then remained stable from later in the afternoon and throughout the night. The optical density measured at 735 nm was stable during the morning chlorophyll accumulation, then increased in the early afternoon toward a peak, followed at dusk by a rapid decline toward the late night steady state. The authors propose that these dynamics largely reflect accumulation and subsequent consumption of glycogen granules. This hypothesis is consistent with the sharp peak of respiration that coincides with the putative hydrocarbon catabolism. In the long-day regimen (LD 16:8), these events may mark the transition from the aerobic photosynthetic metabolism to microaerobic nitrogen metabolism that occurs at dusk, and thus cannot be triggered by the darkness that comes later. Rather, control is likely to originate in the circadian clock signaling an approaching night. To explore the dynamics of the link between respiration and circadian oscillations, the authors extrapolated an earlier model of the KaiABC oscillator from *Synechococcus elongatus* to *Cyanothece* sp. The measured peak of respiratory activity at dusk correlated strongly in its timing and time width with the modeled peak in accumulation of the $KaiB_4$ complex, which marks the late afternoon phase of the circadian clock. The authors propose a hypothesis that high levels of $KaiB_4$ (or of its *Cyanothece* sp. analog) trigger the glycogen catabolism that is reflected in the experiments in the respiratory peak. The degree of the correlation between the modeled $KaiB_4$ dynamics and the dynamics of experimentally measured peaks of respiratory activity was further tested during the half-circadian regimen (LD 6:6). The model predicted an irregular pattern of the KaiABC oscillator, quite unlike mechanical or electrical clock pacemakers that are strongly damped when driven at double their endogenous frequency. This highly unusual dynamic pattern was confirmed experimentally, supporting strongly the validity of the circadian model and of the proposed direct link to respiration.

Key words circadian clock, cyanobacteria, model, photosynthesis, respiration

1. To whom all correspondence should be addressed: Ladislav Nedbal, Institute of Systems Biology and Ecology ASCR, Zámek 136, CZ-37333 Nové Hrady, Czech Republic; e-mail: nedbal@greentech.cz.

JOURNAL OF BIOLOGICAL RHYTHMS, Vol. 24 No. 4, August 2009 295-303
DOI: 10.1177/0748730409338367

Cyanobacteria is a phylum of diverse photosynthetic microorganisms that, unlike other photosynthetic prokaryotes, are able to use water as the primary electron donor for photosynthetic electron transport. This ability combined with assimilation of carbon dioxide makes the cyanobacteria, along with similarly oxygenic eukaryotic algae, candidates for the photosynthetic production of biofuels (Chisti, 2007). The successful use of the cyanobacteria as hosts for biofuel production will require a thorough optimization of numerous metabolic processes. A notable issue with the regulation of cyanobacterial metabolism is the circadian rhythm of many processes (Ditty et al., 2003). In particular, the operation of photosynthesis (Ort and Yocum, 1996) and respiration (Schmetterer and Pils, 2004) are under circadian control (Johnson and Golden, 1999), and the coordinate regulation of these 2 processes is an essential determinant of the overall energy balance. We need to understand how metabolism is regulated within the circadian cycle. This study is aimed at the circadian dynamics of photosynthesis, respiration, and growth in the cyanobacterium *Cyanothece* sp. ATCC 51142.

The unicellular cyanobacterium *Cyanothece* sp. ATCC 51142 is remarkable for its capacity to perform photosynthetic energy conversion and nitrogen fixation in the same cell. Photosynthesis and nitrogen fixation are usually mutually exclusive processes: photosynthesis releasing large amounts of molecular oxygen, and nitrogenase activity requiring a low-oxygen (microaerobic) condition (Fay, 1992; Gallon, 1992). In multicellular filamentous cyanobacteria, the incompatibility of oxygenic photosynthesis and microaerobic nitrogen fixation is solved by spatial separation into vegetative oxygen-evolving cells and oxygen-impermeable heterocysts that perform nitrogen fixation (Adams, 2000; Böhme, 1998). This solution is not possible in the unicellular *Cyanothece* sp. ATCC 51142 where it is replaced by separation of the 2 processes in time: photosynthesis during the day and nitrogen fixation at night (Berman-Frank et al., 2003; Sherman et al., 1998). The transition requires tight control over diurnal rhythms that is facilitated by a circadian clock (Johnson and Golden, 1999). The cyanobacterial circadian clock consists of a pacemaker oscillator with input pathways that adjust the endogenous time of the oscillator to solar day time, and output pathways that exert control of gene transcription in synchrony with the particular phase of the solar day (Ditty et al., 2003). In this way it is possible, for example, to initiate processes that prepare for the onset of nitrogen fixation well before the night comes.

The interaction between metabolism and the circadian clock is investigated here by comparing detailed measurements of photosynthesis and respiratory dynamics (Červený et al., 2009; Nedbal et al., 2008) with predictions of the circadian clock model that were developed by Miyoshi et al. (2007).

MATERIALS AND METHODS

Cyanobacteria

The unicellular nitrogen fixing cyanobacterium *Cyanothece* sp. ATCC 51142 (Meunier et al., 1998; Sherman et al., 1998; Schneegurt et al., 1997a) was cultured in artificial ASP2 sea water medium (Provasoli et al., 1957) as modified by van Baalen (1962) without nitrate. The pH of the medium was buffered at pH 8.0 using 15 mM TAPS biological buffer and temperature was stabilized at 30 ± 0.2 °C. Prior to the experiments, inoculum culture was grown in 250-ml Erlenmeyer flasks on an orbital shaker at 30 °C and 35 μmol (photons) $\cdot m^{-2} \cdot s^{-1}$ of photosynthetically active radiation (PAR) provided by fluorescent lamps.

Bioreactor

The cyanobacteria were cultivated, and their growth and metabolism monitored, in a modified FMT-150 bioreactor (Photon Systems Instruments, Brno, Czech Republic). The original instrument was described by Nedbal et al. (2008). The capabilities of the bioreactor were expanded by including gas mixing and gas analyzing utilities, and by incorporation of electrodes for measuring the levels of CO_2 and O_2 dissolved in the cyanobacterial suspension (Červený et al., 2009). The suspension was contained in a flat rectangular cuvette with front and back windows made of glass plates (0.1 × 0.2 m). The cuvette was 0.02 m deep (light path) containing typically 0.35 L of cyanobacterial suspension with temperature control by a Peltier thermocouple in the bottom of the cuvette. The detachable cuvette lid accommodated a pH/T sensor (InPro3250), Clark-type electrode (InPro6800), and pCO_2 electrode. All the electrodes were products of Mettler-Toledo, Inc. (Columbus, OH). The front window of the cuvette was illuminated by an LED array consisting of 12 rows: each row with 4 blue LEDs ($\lambda_{max} \approx 455$ nm, $\Delta\lambda_{1/2} \approx 20$ nm) interlaced with 4 orange LEDs ($\lambda_{max} \approx 627$

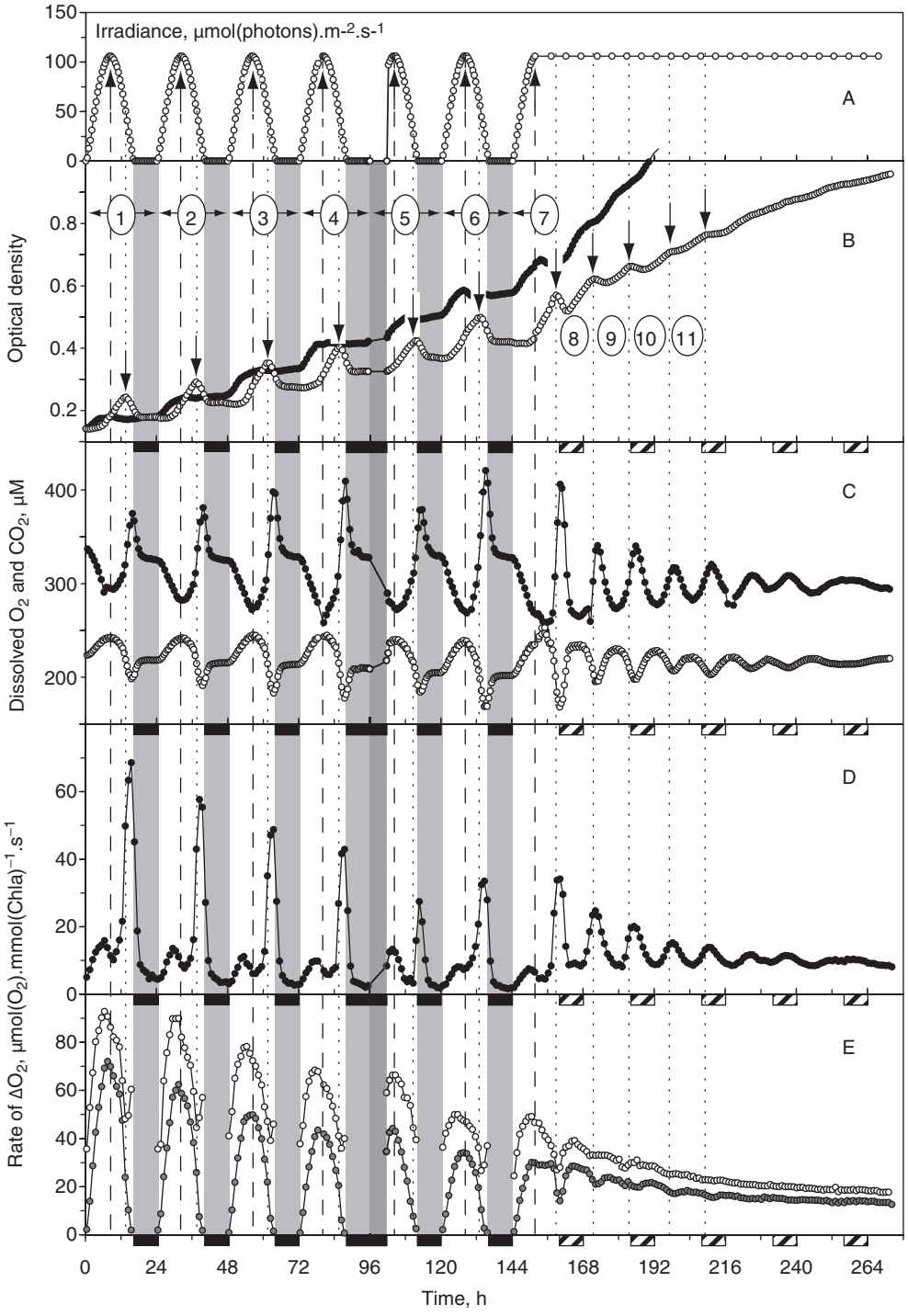

Figure 1. Dynamics of growth and of gas exchange in *Cyanothece* sp. culture with the LD 16:8 forcing (left side) and in the free-running mode of continuous illumination (LL, right side without the vertical gray stripes). (A) Photosynthetically active photon flux density in 24-h periods, numbered 1 to 6. The vertical dashed lines indicate noon with maximum irradiance. The vertical gray bars together with the black horizontal bars on the time axis indicate 8-h long periods of darkness (note the deviation from the regular pattern in the 4th/5th cycles that is commented on in the text). At noon of the 7th day, the light modulation was replaced by constant irradiance to induce the free-run dynamics. The nights would come at periods indicated by hatched horizontal bars. (B) The optical density of the *Cyanothece* sp. suspension at 735 nm (OD_{735}, open circles) and the difference $OD_{680} - OD_{735}$ correlate with biomass and chlorophyll concentration, respectively (Nedbal et al., 2008). The vertical dotted lines and down-pointing arrows show local maxima of OD_{735}. (C) Concentration of O_2 (open circles) and of CO_2 (closed circles) dissolved in the cyanobacterial suspension. (D) Rate of oxygen consumption measured during 3 min of darkness. (E) Rate of oxygen evolution at the bioreactor irradiance level at the time of the measurement (gray filled circles), and at saturating irradiance of 260 μmol (photons) · m^{-2} · s^{-1} (open circles).

nm, $\Delta\lambda_{1/2} \approx 20$ nm). Further details are described in the study by Nedbal et al. (2008). The instrument also stabilized the composition of the CO_2-enriched gas that was bubbled through the suspension. The CO_2 level of the air leaving the cuvette was measured by an infrared monitoring device as described by Červený et al. (2009).

RESULTS

Circadian Forcing and Free Running of Cyanobacterial Metabolism and Growth

Figure 1 represents the dynamics of the *Cyanothece* culture in 2 regimens. First, the culture was forced by six 24-h cycles of 16-h light periods alternating with 8 h of darkness (gray vertical columns). The irradiance dynamics (Fig. 1A) simulated natural solar light during the long northern hemisphere summer day (Bird and Riordan, 1986). The maximum irradiance at noon is indicated in Figure 1 by the vertical dashed lines with up-pointing arrows in panel A. In the 4th cycle, the night lasted longer than intended (dark gray vertical bar starting at the 96th hour of the experiment). We chose to show data from an experiment, including this perturbation to demonstrate the robustness and the

consistency of the cyanobacterial dynamics in the forced 24-h regimen.

In the 2nd part of the experiment at noon of the 7th day the diurnal light modulation was replaced by constant irradiance to investigate the free-running mode of the cyanobacterial dynamics.

Panel B shows measurements of biomass as indicated by optical density (OD_{735}, open circles in Fig. 1B) and measurements of chlorophyll concentration proxy (OD_{680}-OD_{735}, closed circles in Fig. 1B) (Nedbal et al., 2008). The chlorophyll concentration estimated from $OD_{680} - OD_{735}$ starts increasing with the first morning light, stops increasing well before noon, and remains stable until the next morning. The biomass measured by OD_{735} (open circles in Fig. 1B) does not change significantly during the morning hours as the chlorophyll content increases. With the end of the chlorophyll accumulation, the biomass starts to increase, reaching a sharp maximum late in the afternoon. The local maxima of OD_{735} are indicated by vertical dotted lines. These maxima are followed by a rapid decrease, indicating a sharp drop in biomass that ends within the 1st hour of darkness.

The continuous irradiance phase of the experiment resulted in cyanobacterial dynamics with damped local maxima that were only 12 to 13 h apart (Fig. 1B, periods numbered 8 to 11).

Panel C shows the concentration of dissolved CO_2 (closed circles) and of dissolved O_2 (open circles). During the morning hours of the forced 24-h mode, the dissolved CO_2 drops and dissolved O_2 increases due to the dominating effects of photosynthetic O_2 evolution and CO_2 assimilation. As anticipated, these dynamic features peak at noon when the irradiance is at its maximum. The early afternoon decrease in photosynthetic activity can be explained by decreasing irradiance (Fig. 1, panel A). However, this gradual process is abruptly accelerated at the time when the biomass, as measured by OD_{735}, reaches a maximum, as indicated by the dotted vertical line with the down-pointing arrow in panel B of Figure 1. The local maxima of OD_{735} coincide with a sharp increase of dissolved CO_2 and with a drop of dissolved O_2, culminating in the sharp respiratory peak in the late afternoon light, and well before full darkness. With darkness, the dissolved CO_2 and dissolved O_2 converge to steady-state levels that are maintained for the rest of the night.

Panel D in Figure 1 shows the rate of oxygen uptake during approximate 3-min periods when the bubbling of the cyanobacterial suspension is interrupted and lights are switched off (see Fig. 3 in Červený et al., 2009, for details). The respiratory oxygen uptake rises with increasing irradiance in the morning hours, and the maximum is reached well before noon. The depression of the respiratory activity at noon (vertical dashed line) is followed by a dramatic sharp increase that coincides with the maximum in OD_{735} (dotted lines with down-pointing arrows). This sharp respiratory peak is a remarkable dynamic feature that we tentatively interpret as a moment of transition from oxygenic photosynthetic metabolism to microaerobic nitrogen fixation. Interestingly, this moment comes late in the light period in an anticipation of the upcoming dark period. Confirming the result from panel B, the periodicity of the respiratory peaks in the forced diurnal regimen is 24 h, and in the free-running mode is approximately 12 to 13 h. The dumping time constant of respiratory periodic dynamics in the free-running mode is approximately 3 to 4 days.

In contrast to respiration, the photosynthetic oxygen evolution rate (gray filled symbols in Fig. 1E) follows changes in incident irradiance very closely. In the free-running mode, with an exception of the rate dip at around 157th hour of the experiment that comes in an anticipation of upcoming night, the oxygen evolution rate declines steadily. The oxygen evolution rate at the saturating irradiance (open symbols in Fig. 1E) exhibits a local minimum followed by a transient rise just at the time of the respiratory peak. This feature, however, fades away rapidly in the free-running mode.

Column 1 (A-1 to D-1) in Figure 2 shows details of 2 periods of the forced circadian mode that were described in a broader context in Figure 1. Columns 2 and 3 show results obtained with another 2 experimental protocols in which the circadian regimen was forced using the same integral of photons per day as in column 1 but concentrated in shorter light periods and separated by longer nights (vertical gray stripes). Also, in contrast to column 1, in which the light was sinusoidally modulated during the day hours (panel A in Fig. 1), the light in columns 2 and 3 was constant during the day hours.

Despite the substantial differences between the protocols in column 1 and in columns 2 and 3, the overall dynamic patterns in culture optical densities (panel A), in dissolved CO_2 and O_2 (panel B), in respiration rate (panel C), and in photosynthetic O_2 evolution rates (panel D) are similar. The drop in OD_{735}, which follows the maximum during the late afternoon hours of the 16-h day in A-1, occurs at the beginning of night both in A-2 (12-h light day) and in

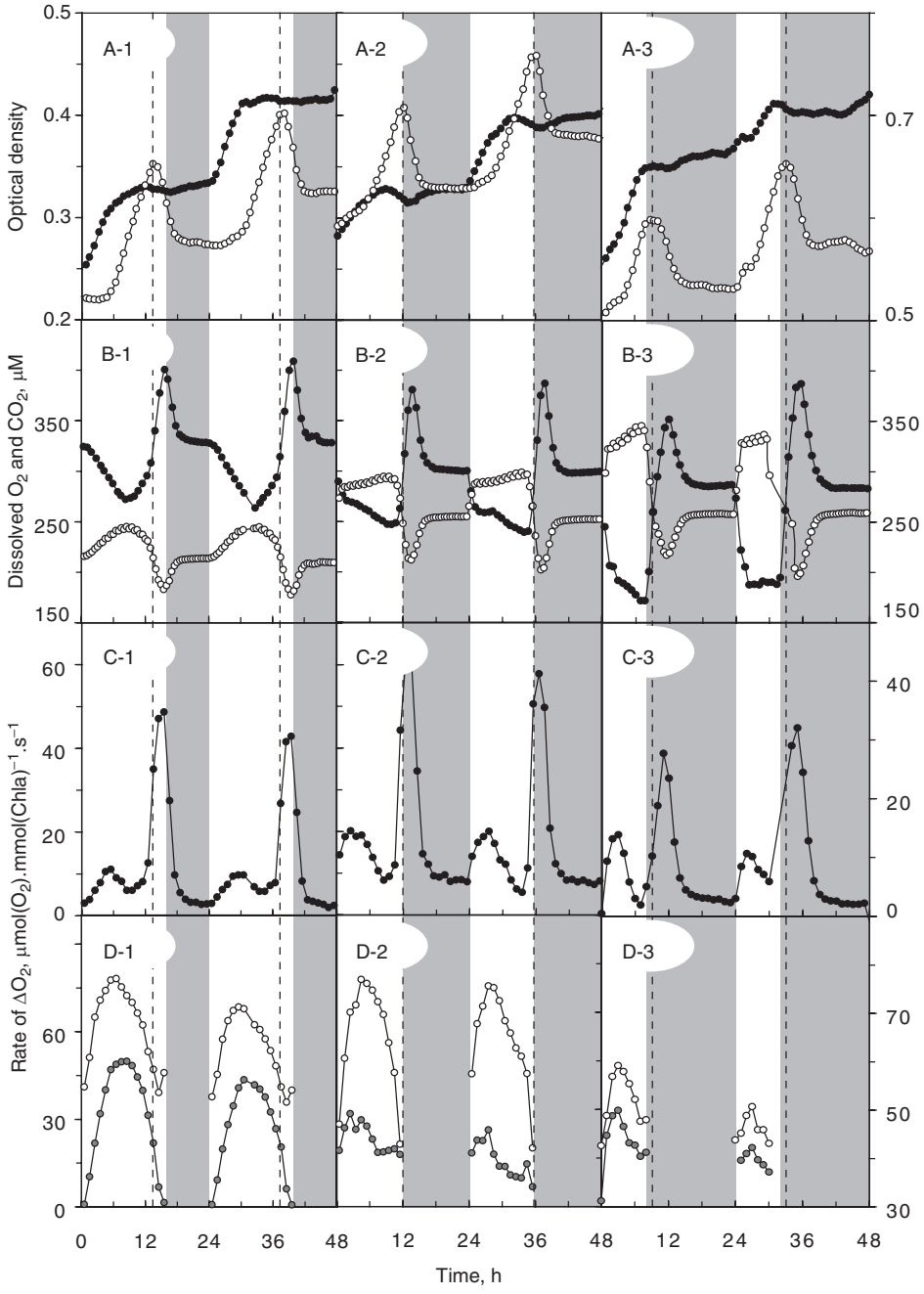

Figure 2. Dynamics of growth and gas exchange during forcing with LD 16:8 (column 1), with LD 12:12 (column 2), and with LD 8:16 (column 3). Column 1 shows in detail 2 periods obtained with the protocol used in Figure 1. Columns 2 and 3 show 2 periods in which the light was kept constant at levels providing the same number of photons per day as in column 1. In column 2, 12 h of constant irradiance was maintained at 91 μmol (photons) · m^{-2} · s^{-1}, and in column 3, 8 h of constant irradiance was maintained at 137 μmol (photons) · m^{-2} · s^{-1}. Row A shows optical densities of the cultures, row B dynamics of concentrations of dissolved O_2 and CO_2, row C respiratory O_2 uptake rate, and row D actual and light-saturated photosynthetic O_2 evolution rate (after subtraction of respiration).

A-3 (8-h light day). Again, we tentatively interpret the maxima in OD_{735} as marking the activation of the respiratory apparatus that utilizes interthylakoidal carbohydrate glycogen granules described by Schneegurt et al. (1997b). The activation is reflected by a sharp increase in dissolved CO_2 and decrease in dissolved O_2 (panel B in Fig. 2), and by a sharp rise of respiratory O_2 uptake rate (panel C in Fig. 2). In all tested protocols, the maxima marking the respiratory peak follow the maxima of OD_{735} with a delay of a few hours.

The afternoon decline of photosynthetic O_2 evolution is much less pronounced (panel D in Fig. 2), indicating that the levels of dissolved O_2 are controlled by respiration rather than photosynthesis.

The differences in the dynamics shown in columns 1, 2, and 3 of Figure 2, although subtle, communicate a great deal of information. The onset of the respiratory peak coincides with the maximum of OD_{735} that occurs in A-1 of Figure 2 in the late afternoon, and well before the light is switched off. We conclude that this event is clock controlled rather than dark triggered. The timing of the clock does not change much with changes in effective irradiance as, for example, in Figure 1 when the culture density grew from below OD_{735} 0.2 to 0.8. The results show that the internal clock controlling the respiratory peak is set to >12 h of light, and can be triggered also by darkness if coming earlier (<12 h). We tentatively propose that the physiological role of the respiratory peak is to generate a microaerobic intracellular environment required for oxygen-sensitive nitrogen fixation.

Model

Figure 3 shows a tentative scheme of interactions between metabolic processes and the circadian clock. The diurnal metabolic cycle refers to *Cyanothece* sp. while the model of the circadian oscillator was derived for another model cyanobacterium, *Synechococcus elongatus*. We assume that the dynamic circadian features in the 2 organisms would be qualitatively similar. The molecular base of the circadian oscillator in cyanobacteria was discovered by Ishiura et al. (1998). During the circadian cycle, the KaiC hexamer ($KaiC_6$) undergoes a phosphorylation and dephosphorylation cycle that measures the endogenous time. The phosphorylation of $KaiC_6$ by ATP is accelerated by the binding of the KaiA dimer ($KaiA_2$) and its dephosphorylation is accelerated by the active form of the KaiB tetramer ($KaiB_4$). Details of cyanobacterial circadian clocks are described in a number of excellent reviews (e.g., Dong and Golden, 2008; Johnson et al., 2008).

The KaiABC pacemaker is synchronized with physical day and night rhythms by input pathways that communicate the state of a yet unknown light sensor. Dong and Golden (2008) suggested that light sensing can be coupled to photosynthesis by mediating the redox state of the quinone pools. In Figure 3 this interaction is indicated by the dotted line arrow that connects the mornings of the metabolic and circadian cycles.

The circadian pacemaker communicates the clock phase (endogenous time) to the organism via a number of output pathway components that are scarcely known in *Synechococcus* (Iwasaki et al., 2000; Takashi Osanai, 2008; Tsinoremas et al., 1996) and not known in *Cyanothece* sp. For the sake of simplicity, we shall only assume the existence of such a link and investigate dynamic homologies between the experimentally measured metabolic cycle and the modeled circadian cycle. There are several recent models of the core KaiABC oscillator (Mori et al., 2007; Rust et al., 2007; van Zon et al., 2007) that reflect in great molecular detail the key features of the circadian clock, such as temperature compensation and robustness (for extensive review, see Ditty et al., 2009). We chose a less detailed model by Miyoshi et al. (2007) that, although based on a relatively simple representation of the core clock, allows simulation of the light-dark forcing *in vivo* with light-enabled gene transcription/translation and protein degradation.

Simulation of KaiABC Dynamics with Circadian Forcing

The dynamic pattern observed experimentally in the cyanobacterial metabolism (Fig. 1) is compared with the circadian clock model prediction in Figure 4. The model by Miyoshi et al. (2007) consists of 13 ordinary differential equations for individual forms of KaiA, KaiB, and KaiC proteins (see Supplementary Online Material). The light-dark forcing was introduced into the model by light-enabled gene transcription/translation and by protein degradation. Figure 4 shows, in its top row, a model simulation of the $KaiA_2$ and $KaiB_4$ compared with respiratory O_2 uptake measured during LD 16:8 (Fig. 4, A-1), LD 12:12 (Fig. 4, A-2), and LD 8:16 (Fig. 4, A-3). There is a striking correlation between the experimentally found respiratory peak and the modeled peak in the active form of $KaiB_4$.

$KaiB_4$ was suggested to facilitate the dephosphorylation of the $KaiC_6$ hexamer at the core of the circadian pacemaker (e.g., Dong and Golden, 2008; Johnson et al., 2008). Indeed, the simulation shows (Fig. 4) that the peaks in $KaiB_4$ coincide with a rapid decline of the phosphorylated hexamer form ($CPKaiC_6$) and antiparallel rise of the non-phosphorylated form ($KaiC_6$).

We suggest that the dephosphorylation of $CPKaiC_6$ and/or the spike in the $KaiB_4$ concentration is very rapidly communicated to metabolic events. This timing signal triggers the sharp peak in respiratory activity that generates the microaerobic environment necessary for nitrogen fixation at night and occurs at dusk in the LD 16:8 regimen (Fig. 2, C-1 and Fig. 4, A-1), around sunset in the LD 12:12 regimen (Fig. 2, C-2 and Fig. 4, A-2) and with only small delay into night in the LD 8:16 regimen (Fig. 2, C-3 and Fig. 4, A-3). A very similar pattern was predicted by the model simulation for $KaiB_4$ peak accumulation.

The coincidence between the peak in respiration rate and that in the $KaiB_4$ cell content was not confirmed in the free-running mode when the respiratory activity showed a dominant peak every approximately 12 to 13 h (Fig. 1D), whereas the KaiABC clock continued to oscillate with a circadian period of approximately 24 h (Miyoshi et al., 2007).

Correspondence between the Experimentally Observed Metabolic Patterns and Circadian Model Was Challenged by Imposing LD 6:6 Half-Circadian Rhythm

The dynamic correspondence between the experimentally observed respiratory peak and the

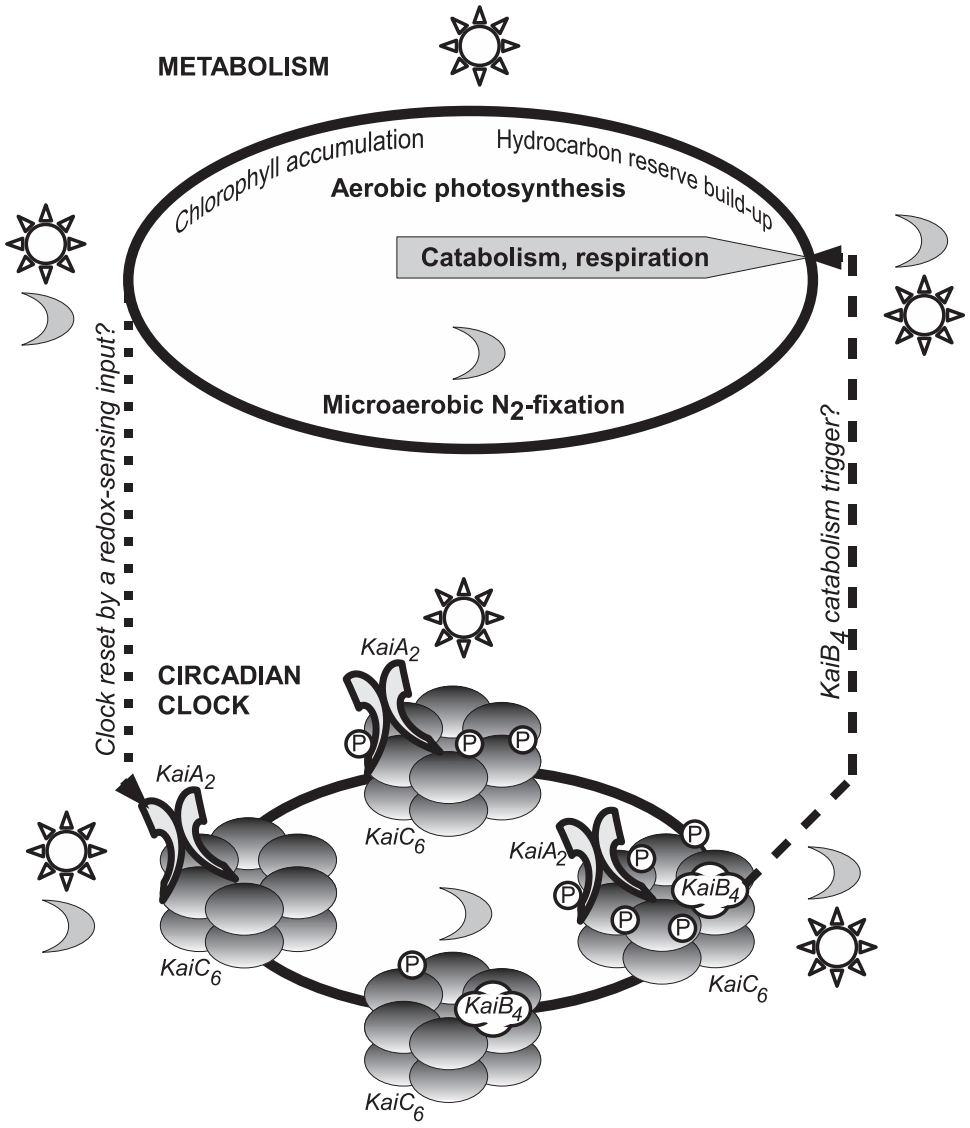

Figure 3. A scheme of the circadian KaiABC clock oscillator (bottom part) and of the daily cycle of the *Cyanothece* metabolism (top part). The circadian scheme conforms with the model in Mackey and Golden (2007). The reset of the circadian clock by a redox sensing of quinone pools indicated by the dotted line arrow was adopted from Dong and Golden (2008). These models are derived for the cyanobacterial model organism *Synechococcus elongatus*. Our results presented in Figure 4 can be largely explained by a putative trigger signal that is directly connecting intracellular levels of the $KaiB_4$ protein to the intense respiratory pulse in dusk (the dashed line arrow).

model-predicted peak in $KaiB_4$ concentration was preserved with various LD ratios (Fig. 2). Yet one cannot exclude that the correspondence of these 2 sharp dynamic features is coincidental. To reduce the likelihood of a purely coincidental correlation, we probed the prediction of the model in a highly unusual periodic pattern with 6 h of light and 6 h of dark. Linear mechanical or electric oscillators are predicted to respond to an off-resonance forcing by a strongly damped oscillation. The model of Miyoshi et al. (2007) predicted irregular KaiABC dynamics: The peaks in the $KaiB_4$ concentration were predicted with apparently random, but not significantly damped amplitudes. Also, the timing of their appearance was predicted to be largely random, sometimes 1 peak per period, sometimes none (see the Supplementary Online Material, Fig. S1). Since this prediction could be an artifact of numerical simulation, we tested the simulation result with experimental observations. Confirming the model prediction, the characteristic respiratory peaks continued to appear, but both the amplitude and the number of peaks per 24 h were variable (see the Supplementary Online Material, Fig. S2). That the qualitative agreement was confirmed by experiment strongly supports the validity of the model.

DISCUSSION

Our results showed that in the long-day experiment (LD 16:8), the rapid drop in the 735-nm optical density (Fig. 1B), and the sharp peak of respiratory activity (Fig. 1D), occur at the end of the day, but still in the light period. Clearly, this phenomenon is controlled by a circadian clock rather than by the onset of darkness. We propose that the drop in the suspension optical density at dusk reflects the disintegration of glycogen granules that represent stored energy from the period of high photosynthetic activity earlier in the day (Fig. 1E). The catabolic activity reflected in the peak of respiratory O_2 uptake (Fig. 1D) may contribute to creating the microaerobic environment required for

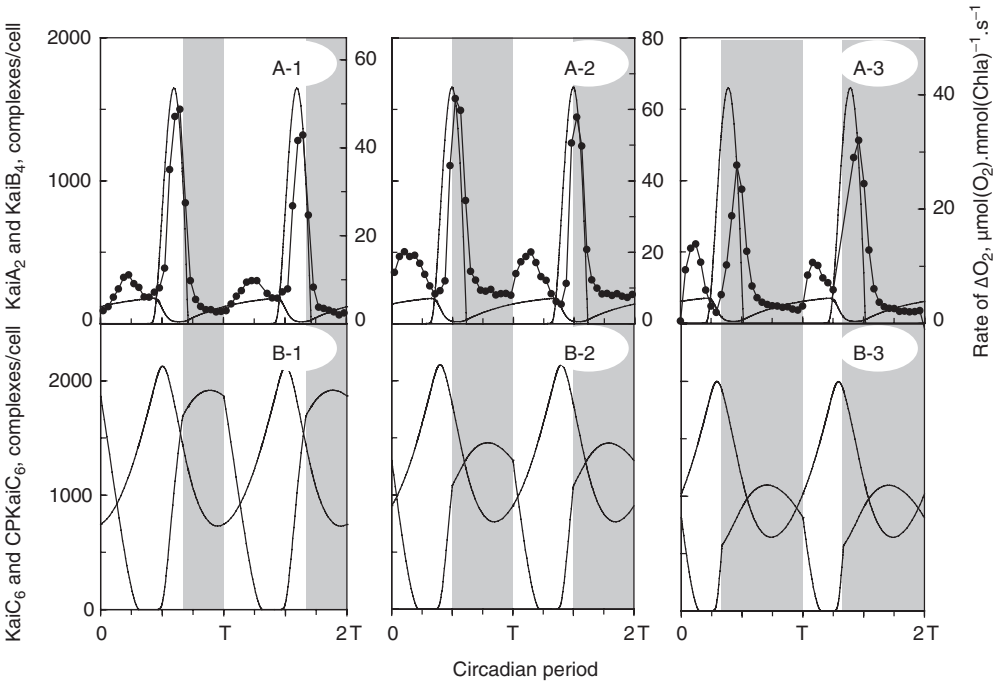

Figure 4. Simulated dynamics of the $KaiA_2$ (A panels, thin lines) and $KaiB_4$ complexes (A panels, heavy lines) compared with measured respiratory O_2 uptake (A panels, closed circles) in the LD 16:8 (A-1), LD 12:12 (A-2), and LD 8:16 regimens (A-3). The dynamics of the nonphosphorylated $KaiC_6$ (B, thin lines) and the fully phosphorylated $CPKaiC_6$ (B, heavy lines) hexamer complexes are shown in the B row of panels.

nitrogenase activity during the night. This transition is also reflected in the changing concentration of dissolved O_2 in the suspension (Fig. 1C). Remarkably, the rate of photosynthetic O_2 evolution (Fig. 1E, gray filled circles) is largely unaffected by these circadian phenomena, and follows approximately the daily irradiance pattern (Fig. 1A). An exception is that the light-saturated O_2 rate shows a depression in the dusk phase (Fig. 1E, open circles) that indicates a down-regulation of photosynthetic activity with the transition to nitrogen metabolism in the late afternoon.

The simulation results in Figure 4A show a strong correlation between the presumed catabolic event marked by the peak in respiratory activity, and the simulated dynamics of the $KaiB_4$ complex in the circadian pacemaker. A causal relationship between these 2 events is suggested because $KaiB_4$ facilitates dephosphorylation of $CPKaiC_6$ (e.g., Dong and Golden, 2008; Johnson et al., 2008), which is known to signal the upcoming night of the circadian clock (Fig. 4B).

Our conclusions rely, in part, on use of the circadian clock model by Miyoshi et al. (2007) that was derived for *Synechococcus elongatus* rather than for *Cyanothece* sp. The validity of the model was challenged in a simulation of KaiABC dynamics during half-circadian (T = ~12 h) forcing of LD 6:6. The model predicted irregular occurrence of $KaiB_4$ accumulation events rather than damping. In correlating $KaiB_4$ level with respiratory peaks, one might expect that during experiments with the LD 6:6 regimen both would show a similar random pattern. Indeed, we found a qualitative agreement between the simulated and measured irregular dynamic patterns of $KaiB_4$ and of respiratory O_2 uptake, respectively, and we interpret this agreement as a validation of the Miyoshi model.

We propose a hypothesis that respiration is controlled by the circadian clock via a direct and nearly instantaneous interaction with the active protein tetramer $KaiB_4$ (or with a *Cyanothece* $KaiB_4$ analog). The hypothesis is based on the robust correspondence between the experimentally observed respiratory peak and the modeled $KaiB_4$ abundance. This model-based hypothesis must be verified by linking the respiratory peak to the experimentally measured concentration of the active $KaiB_4$ tetramer.

ACKNOWLEDGMENTS

The authors were supported by grant AV0Z608-70520 (Czech Academy of Sciences) and by GAČR 206/09/1284 (Czech Science Foundation). LN was also supported by Photon Systems Instruments, Ltd. The authors are grateful to Dr. Stephen Hunt of Qubit Systems, CND, to Dr. Jeremy Harbinson of Wageningen University, Netherlands, for critical reading of the manuscript, and to Matt Stone of the University of Mississippi for improving the language.

REFERENCES

Adams DG (2000) Heterocyst formation in cyanobacteria. Curr Opin Microbiol 3:618-624.

Berman-Frank I, Lundgren P, and Falkowski P (2003) Nitrogen fixation and photosynthetic oxygen evolution in cyanobacteria. Res Microbiol 154:157-164.

Bird RE and Riordan C (1986) Simple solar spectral model for direct and diffuse irradiance on horizontal and tilted planes at the Earth's surface for cloudless atmospheres. J Appl Meteorol 25:87-97.

Böhme H (1998) Regulation of nitrogen fixation in heterocyst-forming cyanobacteria. Trends Plant Sci 3:346-351.

Červený J, Šetlík I, Trtílek M, and Nedbal L (2009) Photobioreactor for cultivation and real-time, in-situ measurement of O_2 and CO_2 exchange rates, growth dynamics, and of chlorophyll fluorescence emission of photoautotrophic microorganisms. Eng Life Sci 9:i3.

Chisti Y (2007) Biodiesel from microalgae. Biotechnol Adv 25:294-306.

Ditty JL, Mackey SR, and Johnson CH (2009) *Bacterial Circadian Programs*. Berlin: Springer.

Ditty JL, Williams SB, and Golden SS (2003) A cyanobacterial circadian timing mechanism. Annu Rev Genet 37:513-543.

Dong G and Golden SS (2008) How a cyanobacterium tells time. Curr Opin Microbiol 11:541-546.

Fay P (1992) Oxygen relations of nitrogen fixation in cyanobacteria. Microbiol Rev 56:340-373.

Gallon JR (1992) Reconciling the incompatible—N_2 fixation and O_2. New Phytol 122:571-609.

Ishiura M, Kutsuna S, Aoki S, Iwasaki H, Andersson CR, Tanabe A, Golden SS, Johnson CH, and Kondo T (1998) Expression of a gene cluster *kaiABC* as a circadian feedback process in cyanobacteria. Science 281:1519-1523.

Iwasaki H, Williams SB, Kitayama Y, Ishiura M, Golden SS, and Kondo T (2000) A KaiC-interacting sensory histidine kinase, *sasA*, necessary to sustain robust circadian oscillation in cyanobacteria. Cell 101:223-233.

Johnson CH, Egli M, and Stewart PL (2008) Structural insights into a circadian oscillator. Science 322: 697-701.

Johnson CH and Golden SS (1999) Circadian programs in cyanobacteria: Adaptiveness and mechanism. Annu Rev Microbiol 53:389.

Mackey SR and Golden SS (2007) Winding up the cyanobacterial circadian clock. Trends Microbiol 15:381-388.

Meunier PC, Colon-Lopez MS, and Sherman LA (1998) Photosystem II cyclic heterogeneity and photoactivation in the diazotrophic, unicellular cyanobacterium *Cyanothece* species ATCC 51142. Plant Physiol 116:1551-1562.

Miyoshi F, Nakayama Y, Kaizu K, Iwasaki H, and Tomita M (2007) A mathematical model for the Kai-protein-based chemical oscillator and clock gene expression rhythms in cyanobacteria. J Biol Rhythms 22:69-80.

Mori T, Williams DR, Byrne MO, Qin X, Egli M, McHaourab HS, Stewart PL, and Johnson CH (2007) Elucidating the ticking of an *in vitro* circadian clockwork. PLoS Biol 5:e93.

Nedbal L, Trtílek M, Červený J, Komárek O, and Pakrasi HB (2008) A photobioreactor system for precision cultivation of photoautotrophic microorganisms and for high-content analysis of suspension dynamics. Biotechnol Bioeng 100:902-910.

Ort DR and Yocum CF (1996) *Oxygenic Photosynthesis: The Light Reactions*. Dordrecht: Kluwer Academic Publishers.

Provasoli L, McLaughlin JJA, and Droop MR (1957) The development of artificial media for marine algae. Arch Mikrobiol 25:392-428.

Rust MJ, Markson JS, Lane WS, Fisher DS, and O'Shea EK (2007) Ordered phosphorylation governs oscillation of a three-protein circadian clock. Science 318:809-812.

Schmetterer G and Pils D (2004) Cyanobacterial respiration. In *Respiration in Archaea and Bacteria: Diversity of Prokaryotic Respiratory Systems*, Zannoni D, ed, p 310, Dordrecht, Kluwer Academic Publishers.

Schneegurt MA, Sherman DM, and Sherman LA (1997a) Growth, physiology, and ultrastructure of a diazotrophic cyanobacterium, *Cyanothece* sp. strain ATCC 51142, in mixotrophic and chemoheterotrophic cultures. J Phycol 33:632-642.

Schneegurt MA, Sherman DM, and Sherman LA (1997b) Composition of the carbohydrate granules of the cyanobacterium, *Cyanothece* sp. strain ATCC 51142. Arch Microbiol 167:89-98.

Sherman LA, Meunier P, and Colon-Lopez MS (1998) Diurnal rhythms in metabolism: A day in the life of a unicellular, diazotrophic cyanobacterium. Photosynth Res 58:25-42.

Takashi Osanai MIKT (2008) Group 2 sigma factors in cyanobacteria. Physiol Plant 133:490-506.

Tsinoremas NF, Ishiura M, Kondo T, Anderson CR, Tanaka K, Takahashi H, Johnson CH, and Golden SS (1996) A sigma factor that modifies the circadian expression of a subset of genes in cyanobacteria. EMBO J 15: 2488-2495.

van Baalen C (1962) Studies on marine blue-green algae. Bot Mar 4:129-139.

van Zon JS, Lubensky DK, Altena PRH, and ten Wolde PR (2007) An allosteric model of circadian KaiC phosphorylation. Proc Natl Acad Sci U S A 104: 7420-7425.